

# Photoelectron spectroscopy of $C_4H_4^-$ : *Ab initio* calculations and dynamics of the 1,2-hydrogen shift in vinylvinylidene

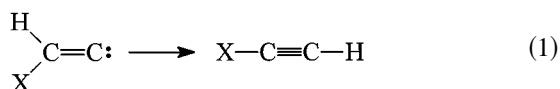
Robert F. Gunion, Horst Köppel,<sup>a)</sup> Gary W. Leach,<sup>b)</sup> and W. C. Lineberger  
*JILA and Department of Chemistry and Biochemistry, University of Colorado, Boulder, Colorado 80309*

(Received 1 February 1995; accepted 19 April 1995)

The ultraviolet photoelectron spectrum of  $HXC=C^-$  ( $X=C_2H_3$ ) is reported along with *ab initio* calculations. The adiabatic electron affinity of the  $X^1A'$  state is measured to be 0.914(15) eV for  $C_4H_4$  and 0.909(15) eV for  $C_4D_4$ . The term energy of the  $C_4H_4 \tilde{a}^3A'$  state is 1.923(15) eV and the  $b^3A''$  term energy is 2.035(30) eV. Geometries and frequencies of several stationary points on the  $C_4H_4$  and  $C_4D_4$  neutral and anion surfaces at the configuration interaction with singles and doubles level of theory are reported, as well as an intrinsic reaction coordinate calculation at the restricted Hartree Fock level on the  $C_4H_4$  singlet surface. Calculations and experiment are combined to estimate the lifetime of singlet vinylvinylidene for rearrangement to vinylacetylene to be 20–200 fs, corresponding to lifetime broadening of 35–3 meV. © 1995 American Institute of Physics.

## I. INTRODUCTION

Several techniques have been pioneered in recent years for studying processes which occur on the subpicosecond timescale. Negative-ion photodetachment has proven especially useful for investigations of transition states<sup>1</sup> and transient species. One such process, the 1,2-hydrogen shift reaction [Eq. (1)], has been the subject of several studies using negative-ion photoelectron spectroscopy [ $X=H^2$  and  $X=F^3$  in Eq. (1)]. Extensive *ab initio* calculations performed concurrently by the Schaefer group<sup>4,5</sup> provided essential additional information on these systems.



The first study, which concentrated on the vinylidene to acetylene ( $X=H$ ) rearrangement,<sup>2,4</sup> analyzes the photoelectron spectrum of  $H_2CC^-$  to estimate the lifetime of the vinylidene singlet ground state to be 0.04–0.2 ps; the rearrangement barrier is  $2 \pm 1$  kcal/mole. The fluorovinylidene to fluoroacetylene ( $X=F$ ) rearrangement<sup>3,5</sup> was found to have a similar barrier to rearrangement. With this exploration of the vinylvinylidene ( $X=C_2H_3$ ) system we continue our previous work and that of others (including at least one very recent article<sup>6</sup>) toward understanding the very fast 1,2-hydrogen shift rearrangements which occur in carbenes, nitrenes, and vinylidenes upon electron detachment from the corresponding anions.

The anion photoelectron spectra reflect the Franck–Condon overlap of anion and neutral wave functions at the anion equilibrium geometry. In this process, an anion absorbs a photon whose energy is greater than the binding energy of the extra electron (eBE); the electron is released with some kinetic energy (eKE) related to the binding energy (eKE =  $h\nu - eBe$ ). The electron departs the anion with a velocity<sup>2</sup> on the

order of 10 Å/fs, and thus the nuclear frame is rigid on the time scale for the electron to be effectively decoupled from the molecular frame. Therefore, in systems where an anion is stable to rearrangement but the corresponding neutral is not, negative-ion photoelectron spectroscopy can probe the early time evolution of the neutral as it rearranges. The use of negative-ion photoelectron spectroscopy to examine these short-lived species is an ideal frequency domain probe of these “transition states,” and represents a valuable complement to time domain probes. In a closely related phenomenon, dissociative states have been observed in the continuous UV spectra of polyatomics<sup>7–9</sup> and the simple interpretation of these spectra was presented by Pack.<sup>10</sup>

The 1,2-hydrogen shift rearrangement<sup>11</sup> [Eq. (1)] is a ubiquitous intramolecular chemical reaction, with vinylidene ( $H_2CC$ ) being the simplest possible example. It is the apparent simplicity of vinylidene, coupled with the generality of the 1,2-hydrogen shift, that has produced extensive theoretical and experimental efforts to understand the dynamics involved in this process. The barrier to the 1,2-hydrogen shift rearrangement in the anion is relatively high (40–50 kcal/mole),<sup>12–18</sup> as it is in the lowest lying triplet state of the neutral.<sup>19</sup> The singlet ground state of the neutral, however, has an empty orbital on the terminal carbon to which the hydrogen atom on the adjacent carbon can migrate, making the barrier to isomerization very small. A very clear explanation of the difference in singlet, anion, and triplet isomerization barriers is contained in Harding’s 1981 treatment of the 1,2-hydrogen shift.<sup>18</sup> This barrier has been the subject of intense theoretical and experimental investigations. The first extensive *ab initio* investigation<sup>15</sup> of the vinylidene singlet surface was published by Schaefer’s group, who found a barrier to rearrangement of 5–8 kcal/mole. In 1981 two sets of calculations were published for this system with contradictory findings: at the MP2 and MP4 levels of theory, no minimum corresponding to singlet vinylidene was found,<sup>20</sup> while the Schaefer group published improved calculations<sup>16</sup> which lowered their estimate of the classical rearrangement barrier to 4 kcal/mole. The latest vinylidene calculation by

<sup>a)</sup>JILA Visiting Fellow, 1993–94; permanent address: Theoretische Chemie, Universität Heidelberg, INF 253, 69120 Heidelberg, Germany.

<sup>b)</sup>Present address: Department of Chemistry, Simon Fraser University, Burnaby, British Columbia, Canada V5A 1S6.



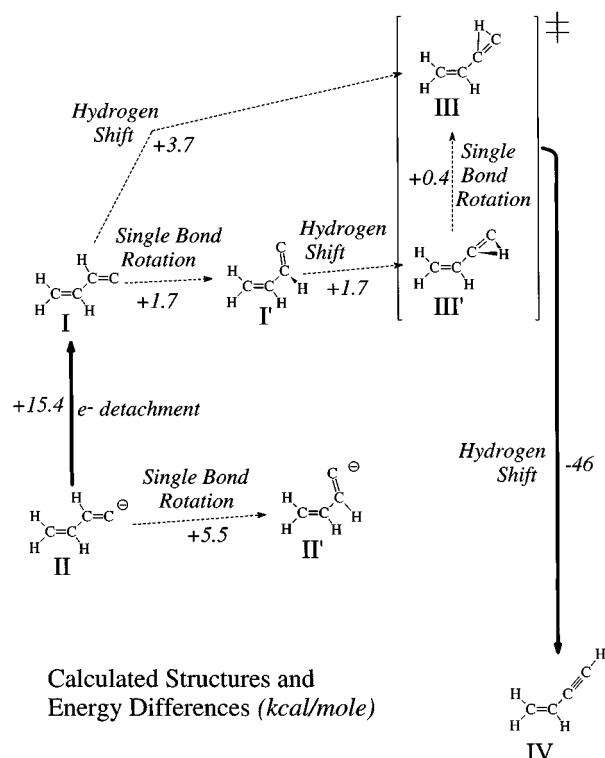
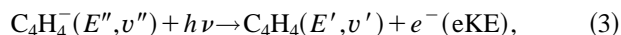


FIG. 1. Stationary points calculated at the CISD level. Relative energies are indicated in kcal/mole. The experimental electron affinity (21.2 kcal/mole) is the preferred value but the CISD result is shown for consistency.

dent on the ions. Photodetached electrons are passed through a hemispherical energy analyzer and focused onto a position sensitive detector. The electron energy resolution is typically 6 meV. The detached electron kinetic energy (eKE) is equal to the photon energy minus the energy difference between initial and final states of the molecule in the process:



where  $(E'',v'')$  refers to the anion electronic and vibrational state, and  $(E',v')$  refers to the electronic and vibrational states of the neutral product. All observed transitions originate from the ground electronic state of the anion. The electron kinetic energy spectrum is thus a series of peaks corresponding to the differences in energy between various vibrational states of the anion and the neutral, with intensities of the peaks determined by Franck–Condon factors.

*Ab initio* calculations were performed in conjunction with the experimental work to help interpret the spectra. The GAUSSIAN92 program was used for most of the calculations.<sup>40</sup> Restricted Hartree Fock (RHF) and configuration interaction with singles and doubles substitutions (CISD) methods were used to obtain geometries at the stationary points indicated in Fig. 1: singlet vinylvinylidene (**I** and **I'**); vinylvinylidene anion (**II** and **II'**); transition state structures (**III** and **III'**); and vinylacetylene (**IV**). An IRC was calculated at the RHF level of theory for the neutral potential energy surface. In addition, single-point calculations were performed at the CISD level at unit normal coordinate displacements of singlet vinylvinylidene, starting from the anion geometry obtained at the CISD level of theory. All calculations employed

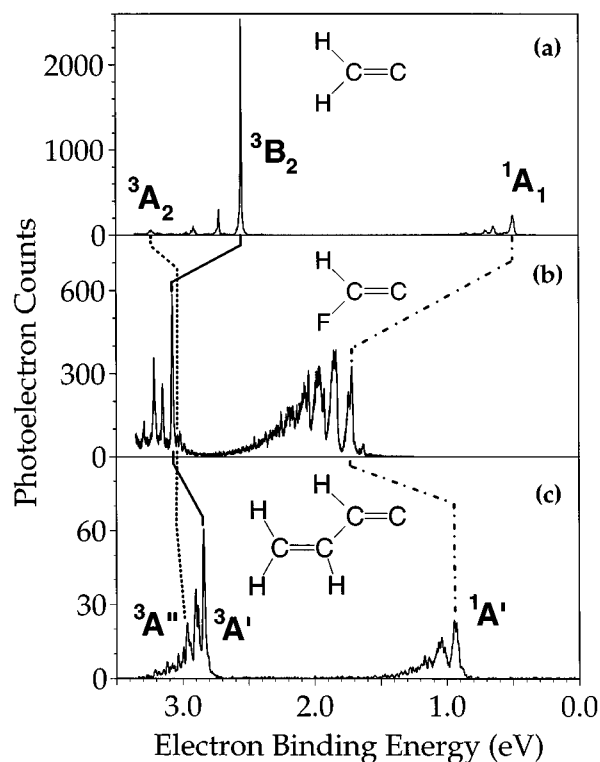


FIG. 2. Overview of the (a) vinylidene, (b) fluorovinylidene, and (c) vinylvinylidene anions 351 nm photoelectron spectra. The origins of the singlet ground states and two triplet excited states are labeled and their relationships indicated by lines. Spectra (a) and (b) are adapted from Refs. 2 and 3, respectively.

a  $\text{DZP}(d,p)$  basis for the neutral, augmented with diffuse functions for the anion. These basis sets are referred to below as  $\text{D95}(d,p)$  and  $\text{D95}++(d,p)$ , respectively. The calculations were performed on a Cray Y/MP4E/232, operating under the UNICOS operating system version 7.0.5.1. The results of these calculations are extensive and only the essential pieces of information are presented here; the balance of the computational results is available as supplementary material.

### III. RESULTS

#### A. Experiment

##### 1. General observations

Figure 2 depicts the 351 nm photoelectron spectra of vinylidene,<sup>2</sup> fluorovinylidene,<sup>3</sup> and vinylvinylidene anions. Table I lists the corresponding electron binding energies, excitation energies, and anisotropy parameters obtained for the electronic states of each species in Fig. 2. The vinylidene spectrum and parameters are adapted from Ervin *et al.*<sup>2</sup> while those of fluorovinylidene are from Gilles *et al.*<sup>3</sup> The similarity of the three spectra is striking, as discussed below.

The vinylidene spectrum [Fig. 2(a)] shows transitions to three electronic states, the origins of which are labeled. The most prominent peak appears at an electron binding energy of 2.555 eV and was assigned to the origin of the  ${}^3B_2$  state by Ervin *et al.*<sup>2</sup> The binding energy of the feature to the right side of Fig. 2(a), the  $\tilde{X}{}^1A_1$  state of the neutral, is the adia-

TABLE I. Electron binding energies, term energies, and anisotropy parameters for the observed vinylidene, fluorovinylidene, and vinylvinylidene electronic states.

Electronic state	Electron Binding energy (eV)	Term energy (eV)	Anisotropy parameter $\beta$ for 351 nm excitation
<b>H<sub>2</sub>CC (Ref. 2)</b>			
$\tilde{X}^1A_1$	0.490(6)	0.0	-0.51(5)
$\tilde{a}^3B_2$	2.555(6)	2.065(6)	+1.45(5)
$\tilde{b}^3A_2$	3.244(6)	2.754(20)	-0.5(2)
<b>HFCC (Ref. 3)</b>			
$\tilde{X}^1A'$	1.718(6)	0.0	
$\tilde{b}^3A'$	3.076(9)	1.358(9)	+1.1(2)
$\tilde{a}^3A''$	3.038(9)	1.320(9)	(undet.)
<b>C<sub>4</sub>H<sub>4</sub> (this work)</b>			
$\tilde{X}^1A'$	0.914(15)	0.0	-0.10(5)
$\tilde{a}^3A'$	2.837(6)	1.923(15)	+0.95(5)
$\tilde{b}^3A''$	2.949(20)	2.035(30)	$\sim -0.1$

batic electron affinity of vinylidene (0.490 eV). The electronic state with the smallest photodetachment cross section appears at 3.244 eV. The assignment of this last peak as a different electronic state was not immediately obvious but was conclusively supported by a dramatic change in the anisotropy parameter of the detached electron, to be discussed below. A few more peaks appear to the left (higher binding energy) side of the  $\tilde{X}^1A_1$  and  $\tilde{a}^3B_2$  origins; these result from transitions to excited vibrational levels of the corresponding neutral electronic states. The origin of each electronic state is much more prominent than the corresponding vibrational overtones, indicating a relatively minor displacement along the normal coordinates of the vibrations. The widths of the peaks, as indicated in Ervin *et al.*,<sup>2</sup> are approximately 24 meV in the ground state and 12 meV in each of the excited states.

The spectrum of fluorovinylidene [Fig. 2(b)] also shows transitions to three electronic states and displays a striking similarity to that of vinylidene. The most prominent peak, at 3.076 eV binding energy, corresponds to a transition to the  $^3A'$  state, similar to vinylidene both in appearance and placement on the binding energy scale. The position of the ground-state origin (assigned by Gilles *et al.*<sup>3</sup> as  $^1A'$ ) gives an adiabatic electron affinity of 1.718 eV, significantly higher than vinylidene as a result of the fluorine substitution. Another excited state ( $^3A''$ ) appears at 3.038 eV. The  $^3A''$  state has a small photodetachment cross section and is indistinguishable from the  $^3A'$  state except with additional information. The electron binding energies of the triplet states are similar to those of the vinylidene triplet states. The width of the  $^3A'$  origin peak is similar to the vinylidene  $^3B_2$  state origin; a comparison of the widths of the peaks in the vinylidene and fluorovinylidene singlet states is complicated by vibrational congestion in the fluorovinylidene singlet state. Except for the increase in the electron affinity and the degree of vibrational excitation, the fluorovinylidene spectrum is remarkably similar to the vinylidene spectrum.

The vinylvinylidene photoelectron spectrum shown in

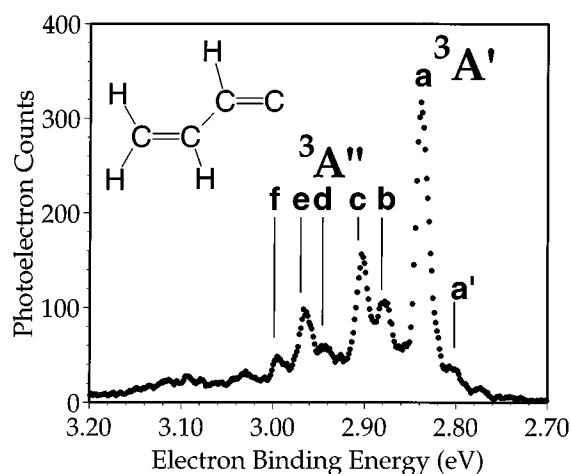


FIG. 3. Detail of the photoelectron spectrum of vinylvinylidene anion, showing the  $\tilde{a}^3A'$  and  $\tilde{b}^3A''$  states. Assignments of peaks  $a'$  and  $a$ - $f$  are listed in Table II.

Fig. 2c contains features reminiscent of the vinylidene and fluorovinylidene spectra. The most prominent peak has an electron binding energy close to those of the corresponding vinylidene and fluorovinylidene triplet states (Table I). Another state is buried beneath the most prominent state, like the fluorovinylidene case, and would be undetectable without additional information. The ground state appears at an electron binding energy just slightly greater than that of vinylidene. The origin of the prominent excited state is narrow (15 meV in this case) while the origin of the ground state is much broader. With so many features common to the vinylidene, fluorovinylidene, and vinylvinylidene spectra, the electronic states present in the vinylvinylidene spectrum can be readily assigned to the symmetries listed in Table I. Full analysis of the spectrum is reflected in Table I; the assignment of the  $^3A''$  state requires polarization data, to be discussed below, and the adiabatic electron affinity cannot be firmly assigned without the considerations appearing in Sec. IV.

The trends apparent in the binding energies of each electronic state in the three spectra also permit some generalization of electronic state energy levels in vinylidene systems. The electron affinities of the three species vary widely from 0.490 to 1.718 eV, indicating that this parameter is heavily dependent on the electronegativity of substituent X. However, the electron binding energies associated with the triplet states change very little from one species to the next, despite their reversal in the fluorovinylidene case (Table I). Therefore the energies of the orbitals from which the extra electron is detached to form these triplet states are fairly independent of the substituent, relative to the anion. The singlet-triplet splittings reflected in Table I vary widely only as a result of the change in electron affinities.

## 2. Triplets

The photoelectron spectra presented in Figs. 2, 3, and 4 were obtained with the angle between the laser electric field vector and the electron collection direction set at the "magic

TABLE II. Positions, anisotropy parameters, and assignments for the peaks labeled in Fig. 3.

Peak	Position (cm <sup>-1</sup> )	Anisotropy parameter $\beta$	Assignment
a'	-250(30)		$\tilde{a}^3A' 1_1^0$
a	0	+0.95	$\tilde{a}^3A' 0_0^0$
b	360(50)	+0.76	$\tilde{a}^3A' 1_1^0$
c	500(50)	+0.45	$\tilde{a}^3A' 2_0^1$
d	835(50)	+0.11	$\tilde{a}^3A'$ and $\tilde{b}^3A''$
e	1,015(50)	-0.05	$\tilde{b}^3A'' 0_0^0$
f	1,250(50)	+0.65	$\tilde{a}^3A' 3_0^1$

angle'' (54.7°), and represent the angle-averaged photodetachment cross section. Additional information can be obtained by examining the corresponding spectra obtained for parallel (0°) and perpendicular (90°) angles of laser polarization to the electron collection direction. The photoelectron angular distribution has the form<sup>41</sup>

$$I(\Theta) \propto 1 + \beta P_2(\cos \theta) \quad (4)$$

with  $-1 < \beta < 2$ ; the anisotropy parameter  $\beta$  for photodetached electrons is estimated with the equation

$$\beta = \frac{I_0 - I_{90}}{(1/2)I_0 + I_{90}}, \quad (5)$$

where  $I_0$  is the intensity of a given peak in the parallel photoelectron detachment spectrum and  $I_{90}$  is the intensity of the same peak for perpendicular detachment. Since the photon contains one unit of angular momentum, the selection rule for photodetachment for atomic orbitals is  $\Delta l = \pm 1$ . Therefore, photodetached electrons originating from  $s$  orbitals show  $p$ -wave detachment ( $\beta=2$ ), while detachment from electrons in  $p$  orbitals results in a mixture of  $s$ - and  $d$ -wave detachment, the relative portions of which are dependent on detachment energy. At the detachment threshold, electrons are pure  $s$  waves, producing isotropic angular distributions ( $\beta=0$ ). At 1–2 eV above threshold,  $d$  waves mix with  $s$  waves and  $\beta$  becomes negative ( $\sin^2 \theta$  distribution). This behavior of the anisotropy parameter is rigorous for atomic photodetachment but for molecules it is more complicated due to the random orientation of the molecular frame. The anisotropy parameter is generally more isotropic, or closer to zero, for molecular detachment. Previous work in our laboratory has shown that  $\beta$  tends to be between 1.5 and 2 for  $s$ -like orbitals in the 0–3 eV electron kinetic energy range, while  $p$ -like orbitals result in  $\beta < 0$  for 1–2 eV electrons.

In the vinylidene and fluorovinylidene studies,<sup>2,3</sup> two triplet states were assigned in the same vicinity as corresponding features in the vinylvinylidene spectrum (Fig. 2 and Table I). These states exhibited significantly different anisotropy parameters, and the angular distribution data allowed a definitive identification; in particular, transitions to the vinylidene  $\tilde{a}^3B_2$  state exhibited a large, positive anisotropy parameter, as did those to the fluorovinylidene  $\tilde{b}^3A'$  state; the anisotropy parameters for the vinylidene  $\tilde{b}^3A_2$  and fluorovinylidene  $\tilde{a}^3A''$  states are negative and closer to zero. These values were used to justify the assignments of the electronic states in the following way: A large positive an-

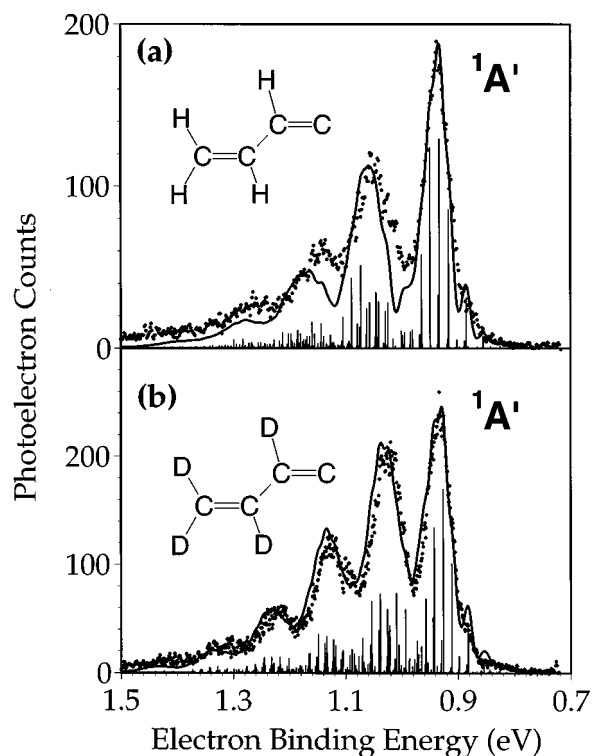


FIG. 4. Detailed view of that portion of the photoelectron spectrum leading to production of the singlet state of vinylvinylidene. (a) Vinylvinylidene- $h_4$ . (b) Vinylvinylidene- $d_4$ . (●) Photoelectron data; (—) Franck–Condon fit; sticks, Franck–Condon line positions and intensities.

isotropy parameter results from  $p$ -wave electrons ( $s$  orbital), consistent with detachment from the carbon lone pair to form the  $^3B_2$  (or  $^3A'$ ) state. A negative anisotropy parameter ( $s$ - and  $d$ -wave electrons) is consistent with detachment from the  $\pi$ -like orbital to form the  $^3A_2$  ( $^3A''$ ) state.

Figure 3 shows the 351 nm photoelectron spectrum of the triplet states of vinylvinylidene with several peaks labeled. The positions of these peaks are included in Table II along with assignments and the anisotropy parameters measured for the transitions from  $v=0$  of the anion (the peak labeled a' is a hot band from a 250(30) cm<sup>-1</sup> anion vibration). Peaks a, b, c, and f show large positive anisotropy parameters, while peak d is considerably more isotropic and  $\beta$  for peak e is negative. By analogy with vinylidene and fluorovinylidene, peaks a–d and f are assigned to the  $\tilde{a}^3A'$  state of vinylvinylidene. Peak a is the origin band, while peaks b, c, and f are assigned to one quantum each of three vibrations at 360(50), 500(50), and 1250(50) cm<sup>-1</sup>, respectively. Peak d is a mixture of the two triplets, while peak e results primarily from the  $\tilde{b}^3A''$  state. The origin of the  $\tilde{b}^3A''$  state is therefore assigned to peak e, with a 30 meV uncertainty in the term energy since the true position of the origin is ambiguous. The angular distribution is also nearly isotropic ( $\beta \approx 0$ ) for the singlet state of vinylvinylidene, consistent with observations for the vinylidene<sup>2</sup> and fluorovinylidene<sup>3</sup> species. The anisotropy parameter for the origin peak of each electronic state in vinylvinylidene is included in Table I; the values from the vinylidene and fluorovinylidene studies are included for comparison.

TABLE III. Parameters obtained for  $\nu_2$ , the  $C_1C_2C_3$  bending vibration close to the isomerization coordinate. The FWHM of Gaussians used to model the spectrum is also included.

	Frequency ( $\text{cm}^{-1}$ )	Anharmonicity ( $\text{cm}^{-1}$ )	Displacement ( $\text{amu}^{1/2}$ bohr)	Gaussian FWHM (eV)
$C_4D_4$				
Calculated	186.6	1.1	1.073	...
Best fit	130	1.1 <sup>a</sup>	0.773	0.017 <sup>b</sup>
$C_4H_4$				
Calculated	196.5	1.2	0.983	...
Best fit	136	1.2 <sup>a</sup>	0.708	0.019 <sup>b</sup>

<sup>a</sup>Constrained to the calculated value.<sup>b</sup>Based on triplet data and further allowed to vary to test effect of lifetime.

### 3. The $\tilde{X}^1A'$ state

Figure 4 displays the singlet state spectra of vinylvinylidene and vinylvinylidene- $d_4$ . Upon a first examination of the data (unconnected symbols), a preliminary electron affinity can be assigned to the center of the origin peak, giving  $EA=0.935$  eV; however, since the width of this peak (52 meV in both  $C_4H_4$  and  $C_4D_4$ ) is an order of magnitude greater than the instrumental resolution, it imposes an uncertainty on the electron affinity of  $\sim 30$  meV. Three distinct peaks are present, evenly spaced at  $\sim 900$   $\text{cm}^{-1}$  in the  $C_4H_4$  spectrum and  $\sim 800$   $\text{cm}^{-1}$  for  $C_4D_4$ ; however, these peaks cannot be assigned to a single vibration since considerable vibrational congestion may be hidden under the large apparent peak widths. *Ab initio* calculations have been used to obtain vibrational frequencies and geometry displacements which were an indispensable aid in the spectral assignment.

The simulated spectrum obtained by combining the results of *ab initio* calculations with minor empirical corrections is included in Fig. 4. Sticks represent the positions and intensities of individual transitions; a Franck–Condon simulation including instrumental, rotational, and lifetime broadening appears as a solid line. The parameters of the simulation are listed in Tables III, IV, and V. A major focus of this paper will be to deconvolute the widths of the singlet spectrum peaks into the separate components of rotational broadening, vibrational congestion, and lifetime broadening. The adiabatic electron affinity can also be measured with greater

TABLE IV. Parameters obtained for higher-frequency modes in vinylvinylidene- $d_4$ . Frequencies are held at 93% of the CISD calculated values.

	Frequency ( $\text{cm}^{-1}$ )	Calculated displacement ( $\text{amu}^{1/2}$ bohr)	Best fit displacement ( $\text{amu}^{1/2}$ bohr)
$\nu_3$ (skeletal rock)	355	0.157	0.120
$\nu_6$ ( $D_5$ rock)	671	0.157	0.220
$\nu_9$ ( $C_2C_3$ stretch)	766	0.128	0.150
$\nu_{10}$ ( $D_5/D_6$ rock)	902	0.126	0.170
$\nu_{13}$ ( $C_1-C_4$ antisymmetric stretch)	1670	0.023	0.080

precision when the full simulation is performed. The results for the singlet spectrum will be addressed more completely in Sec. IV.

## B. Calculations

*Ab initio* calculations using GAUSSIAN92 were carried out on the anion and low-lying singlet states of the neutral molecule in order to assist in the interpretation of the experimental findings. The results of these calculations are presented briefly here, a detailed analysis of their significance to experimental results appears in Sec. IV.

### 1. Geometry optimizations

Calculations at several levels of theory were performed at various stationary points on the  $C_4H_4$  and  $C_4H_4^-$  surfaces. Figure 1 summarizes the relative (CISD) energies of all of these stationary points with the geometrical and electronic transformations relating them to one another. The calculations were performed at the CISD/D95++( $d,p$ ) level for the trans- and cis-vinylvinylidene anion geometries (**II** and **II'**, respectively, Fig. 1) since the inclusion of diffuse functions tends to improve calculations involving anions significantly. The CISD/D95( $d,p$ ) level was used for all other structures in Fig. 1: singlet trans-vinylvinylidene (**I**), singlet out-of-plane vinylvinylidene (**I'**), the transition state between vinylvinylidene and vinylacetylene in the trans (**III**) and out-of-plane (**III'**) configurations, and vinylacetylene (**IV**). The total energies of all complete geometry optimizations, with

TABLE V. Parameters obtained for higher-frequency modes in vinylvinylidene. Frequencies are held at 93% of the CISD calculated values.

	Frequency ( $\text{cm}^{-1}$ )	Calculated displacement ( $\text{amu}^{1/2}$ bohr)	Best fit displacement ( $\text{amu}^{1/2}$ bohr)
$\nu_3$ (skeletal rock)	413	0.138	0.106
$\nu_6$ ( $C_2C_3$ stretch)	876	0.109	0.128
$\nu_8$ ( $H_5$ rock)	915	0.110	0.154
$\nu_{10}$ ( $H_5/H_6$ rock)	1126	0.105	0.141
$\nu_{13}$ ( $C_1-C_4$ antisymmetric stretch)	1695	0.018	0.063

TABLE VI. Total energies of *ab initio* calculations for the vinylvinylidene system (hartrees).

Anion	
ROHF/D95++( <i>d,p</i> ):	-153.687188978
ROHF/6-311++G**:	-153.6953464
CISD/D95++( <i>d,p</i> ):	-154.1577646
Singlet vinylvinylidene	
RHF/D95( <i>d,p</i> ):	-153.6760161
RHF/6-311G**:	-153.679923
CISD/D95( <i>d,p</i> ):	-154.1332741
QCISD/D95( <i>d,p</i> ):	-154.2097514
Transition State	
RHF/D95( <i>d,p</i> ):	-153.6621404
CISD/D95( <i>d,p</i> ):	-154.1279923
Vinylacetylene	
RHF/D95( <i>d,p</i> ):	-153.7357029
CISD/D95( <i>d,p</i> ):	-154.2016392

13 and 14 variables, are included in Table VI; as the highest practicable level of theory the CISD results are used for frequencies and energy differences.

One goal in performing the calculations was to gain insight into the singlet vinylvinylidene photoelectron spectrum. Since this spectrum is effectively a "snapshot" of the neutral at the anion geometry, the geometry of the anion needs to be characterized as completely as possible. Therefore the first step in the calculations is to explore the anion surface using the ROHF and CISD levels of theory. Table VII lists the optimized bond lengths and bond angles for the vinylvinylidene anion (**II**) at the CISD/D95++(*d,p*) level. In this calculation, the dihedral angle which corresponds to rotation about the CC single bond was constrained to 180°, corresponding to the trans isomer; therefore, this minimum could arise simply by symmetry constraints rather than being the true minimum on the anion surface.

To help discount this possibility, a series of geometry optimizations was performed on the anion (also at the ROHF and CISD levels) with dihedral angles at regular intervals from 0° (the cis geometry) to 180°. Optimizations were performed for dihedral angles of 0°, 30°, 60°, 90°, 120°, 150°,

TABLE VII. Geometries of the trans configuration of the vinylvinylidene anion [CISD/D95++(*d,p*)], and of vinylacetylene [CISD/D95(*d,p*): bond lengths (Å) and bond angles (degrees).

Parameter	Anion, <b>II</b> [CISD/D95++( <i>d,p</i> )]	Vinylacetylene, <b>IV</b> [CISD/D95( <i>d,p</i> )]
C <sub>1</sub> -C <sub>2</sub>	1.353 Å	1.209 Å
C <sub>2</sub> -H <sub>5</sub>	1.098	2.272
C <sub>2</sub> -C <sub>3</sub>	1.470	1.445
C <sub>3</sub> -C <sub>4</sub>	1.339	1.338
C <sub>3</sub> -H <sub>6</sub>	1.087	1.081
C <sub>4</sub> -H <sub>7</sub>	1.082	1.079
C <sub>4</sub> -H <sub>8</sub>	1.083	1.079
∠C <sub>1</sub> -C <sub>2</sub> -C <sub>3</sub>	123.0°	178.3°
∠C <sub>1</sub> -C <sub>2</sub> -H <sub>5</sub>	122.2	
∠C <sub>2</sub> -C <sub>1</sub> -H <sub>5</sub>		179.5
∠C <sub>2</sub> -C <sub>3</sub> -C <sub>4</sub>	128.1	123.5
∠C <sub>2</sub> -C <sub>3</sub> -H <sub>6</sub>	117.9	116.3
∠C <sub>3</sub> -C <sub>4</sub> -H <sub>7</sub>	121.5	120.6
∠C <sub>3</sub> -C <sub>4</sub> -H <sub>8</sub>	121.4	121.5

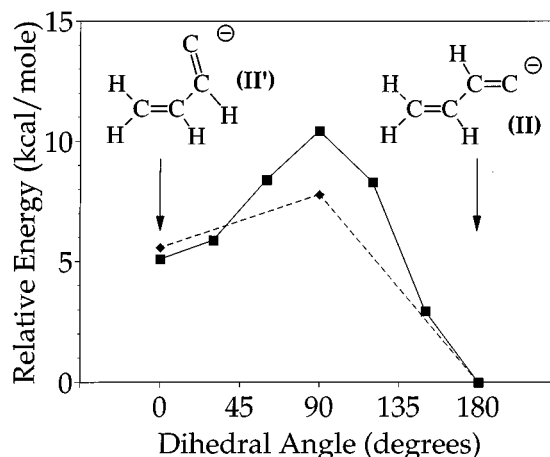


FIG. 5. Variation of the anion *ab initio* total energy with CC single bond rotation (the dihedral angle). (—■—) ROHF/D95++(*d,p*) optimizations every 30°. (---◆---) CISD/D95++(*d,p*) optimizations at 0° and 180°, single-point calculation at 90°.

and 180° at the ROHF level; at the CISD level, the optimizations are at 0° and 180°; the energy at 90° is from a single-point calculation. Smaller steps were not attempted at the CISD level because it reproduced the qualitative trends found at the ROHF level, and the barrier between the two structures appears to maximize near 90°. The relative energies of the anion for the various dihedral angles are depicted in Fig. 5 at the ROHF and CISD levels. The trans structure is a clear minimum at both levels of theory; another minimum occurs at the cis geometry. The *cis*-*trans* isomerization energy is 5.5 kcal/mole at the CISD level, and the CISD barrier to this isomerization is approximately 8 kcal/mole. Though energy differences this small do not entirely preclude the presence of some cis isomers at the thermal temperatures of the photoelectron spectrometer, the absence of apparent contamination in the spectrum (Fig. 2), its similarity to the vinylidene and fluorovinylidene spectra, and the fact that the trans geometry is lower in energy, are further evidence that the species from which the electron is being detached is indeed the trans form of vinylvinylidene anion.

Once the anion geometry is well characterized, the next step is to optimize the geometries at the singlet vinylvinylidene and transition state stationary points. The dihedral angle plays a more complicated role on the neutral potential energy surface than on the anion surface. While the optimized geometry of singlet vinylvinylidene (**I**) has a dihedral angle of 180°, corresponding to a trans planar geometry, the transition state optimization produces a nonplanar structure (**III'**) with a dihedral angle of 68°. A transition state optimization constrained to a planar geometry results in a saddle point of order 2 at the trans configuration (**III**). Another singlet vinylvinylidene (**I'**) is close to the structure of **I**, except the dihedral angle (48°) is close to that of **III'**. The effects of dihedral rotation are most important for an intrinsic reaction coordinate calculation, and are described in more detail in Sec. III B 3. The CISD-optimized bond lengths and angles for the C<sub>4</sub>H<sub>4</sub> stationary points are listed in Table VII (vinylacetylene), Table VIII (singlet vinylvinylidenes), and Table IX (transition states).

TABLE VIII. Geometries of singlet vinylvinylidene calculated at the CISD/D95(*d,p*) level: bond lengths (Å) and bond angles (degrees). The dihedral angle refers to rotation around the CC single bond.

	Planar (trans) I	Nonplanar I'
Dihedral angle	180°	47.7°
C <sub>1</sub> –C <sub>2</sub>	1.314 Å	1.315 Å
C <sub>2</sub> –H <sub>5</sub>	1.091	1.088
C <sub>2</sub> –C <sub>3</sub>	1.471	1.484
C <sub>3</sub> –C <sub>4</sub>	1.338	1.337
C <sub>3</sub> –H <sub>6</sub>	1.081	1.082
C <sub>4</sub> –H <sub>7</sub>	1.079	1.079
C <sub>4</sub> –H <sub>8</sub>	1.080	1.079
∠C <sub>1</sub> –C <sub>2</sub> –C <sub>3</sub>	131.0°	126.0°
∠C <sub>1</sub> –C <sub>2</sub> –H <sub>5</sub>	109.1	113.3
∠C <sub>2</sub> –C <sub>3</sub> –C <sub>4</sub>	123.1	123.9
∠C <sub>2</sub> –C <sub>3</sub> –H <sub>6</sub>	120.2	120.1
∠C <sub>3</sub> –C <sub>4</sub> –H <sub>7</sub>	120.8	120.4
∠C <sub>3</sub> –C <sub>4</sub> –H <sub>8</sub>	121.8	121.7

## 2. Franck–Condon factor calculations

The photoelectron spectrum of the vinylvinylidene singlet state (Fig. 4) is deceptively simple in its appearance. One might think the broad peak widths and short vibrational progression make this an easy spectrum to assign, since the amount of information that can be extracted directly from the spectrum is limited. However, some of the most important information in the spectrum is hidden under the broad peaks, and as such cannot be simply extracted.

*Ab initio* calculations have been used to help identify which vibrations are active in the spectrum, and therefore determine the Franck–Condon factors for the vibrational peaks. The results of the frequency calculations include only four totally symmetric (*A'*) and four nontotally symmetric (*A''*) vibrations under 1000 cm<sup>-1</sup> in structure I. Photoelectron spectroscopy selection rules require that the wave functions associated with active vibrations must be totally symmetric, resulting in transitions of  $\Delta v = 0, \pm 2, \pm 4$ , etc. for *A''*

TABLE IX. Geometries of the transition states of the vinylvinylidene↔vinylacetylene isomerization, calculated at the CISD/D95(*d,p*) level: bond lengths (Å) and bond angles (degrees). The dihedral angle refers to rotation around the CC single bond.

	Planar (trans) III	Nonplanar III'
Dihedral angle	180°	67.66°
C <sub>1</sub> –C <sub>2</sub>	1.261 Å	1.263 Å
C <sub>2</sub> –H <sub>5</sub>	1.409	1.359
C <sub>2</sub> –C <sub>3</sub>	1.447	1.454
C <sub>3</sub> –C <sub>4</sub>	1.337	1.339
C <sub>3</sub> –H <sub>6</sub>	1.081	1.080
C <sub>4</sub> –H <sub>7</sub>	1.078	1.080
C <sub>4</sub> –H <sub>8</sub>	1.079	1.079
∠C <sub>1</sub> –C <sub>2</sub> –C <sub>3</sub>	176.8°	179.0°
∠C <sub>2</sub> –C <sub>1</sub> –H <sub>5</sub>	70.1	68.1
∠C <sub>2</sub> –C <sub>3</sub> –C <sub>4</sub>	125.0	121.4
∠C <sub>2</sub> –C <sub>3</sub> –H <sub>6</sub>	113.9	117.3
∠C <sub>3</sub> –C <sub>4</sub> –H <sub>7</sub>	120.3	120.7
∠C <sub>3</sub> –C <sub>4</sub> –H <sub>8</sub>	122.0	121.4

vibrations; furthermore, Franck–Condon overlaps of these *A''* modes are vanishingly small in the absence of large anharmonicities. Since the vinylvinylidene singlet and the anion are both planar and the *A''* modes involve out-of-plane motion, none of these modes should be active, leaving four vibrations (all with *A'* symmetry) under 1000 cm<sup>-1</sup> possibly active. Two *A'* vibrations,  $\nu_{10}$  at 1126 cm<sup>-1</sup> and  $\nu_{13}$  at 1695 cm<sup>-1</sup> in C<sub>4</sub>H<sub>4</sub>, may contribute a small amount to the photoelectron spectrum and so were included.

The normal coordinates (expressed as displacement vectors of each of the 8 atoms) of these modes were projected onto the CISD-optimized geometry of the trans-vinylvinylidene anion. This produced a series of new geometries on which CISD/D95(*d,p*) single-point energy calculations on the singlet surface were performed. A “map” of the singlet surface at the anion geometry and points displaced along six of the lowest frequency totally symmetric normal coordinates was thus obtained. This facilitated the generation of mass-weighted displacements and anharmonicities (using standard procedures) along these six modes. The mass-weighted displacements are expressed in Tables III–V as a single number in units of amu<sup>1/2</sup> bohr.

The mass-weighted displacements and frequencies for each mode, along with the anharmonicity in  $\nu_2$ , were used as the initial input into a Franck–Condon simulation program, resulting in a simulated spectrum we compared with the experimental data. Minor (with the exception of  $\nu_2$ ) empirical adjustments were made to the displacements, electron affinity, and peak widths to fit the singlet spectrum as well as possible. With this model, the parameters for the H<sub>4</sub> (or D<sub>4</sub>) isotopic species then predict the other spectrum with *no further* adjustable parameters. As one can see in Fig. 4, the vibrational peaks in the photoelectron spectrum of singlet C<sub>4</sub>D<sub>4</sub> are sharper than those in the C<sub>4</sub>H<sub>4</sub> spectrum; for this reason we fit the deuterated spectrum and used the resulting parameters to predict the C<sub>4</sub>H<sub>4</sub> spectrum. The lowest frequency active mode,  $\nu_2$  calculated at 187 cm<sup>-1</sup> (C<sub>4</sub>D<sub>4</sub>), is a C<sub>1</sub>C<sub>2</sub>C<sub>3</sub> bend which lies almost directly along the expected isomerization coordinate, making it not only the most difficult mode to calculate but also the most difficult to model in the spectrum. This mode was treated as a Morse oscillator, while all other normal modes were treated as independent harmonic oscillators. Several simulations were attempted with frequencies of  $\nu_2 = 100, 120, 130, 140, 170$ , and 187 cm<sup>-1</sup>, adjusting the magnitudes of displacements along the normal coordinates and Gaussian peak widths to optimize each. Though all of these simulations accounted for the spectrum almost equally, the fit using 130 cm<sup>-1</sup> was the most successful. The frequencies of the remaining modes ( $\nu_3, \nu_6, \nu_9, \nu_{10}$ , and  $\nu_{13}$ ) were held to 93% of the values calculated at the CISD level. The calculated anharmonicities of these modes are quite small and were neglected. The normal coordinate displacements for these modes required some adjustment but were kept as close as possible to the calculated values. Table III lists the calculated parameters for  $\nu_2$  along with the values obtained in the simulation using  $\nu_2 = 130$  cm<sup>-1</sup>. Table IV contains the calculated frequencies and displacements along with the displacements adjusted empirically for the higher-frequency modes of C<sub>4</sub>D<sub>4</sub>.

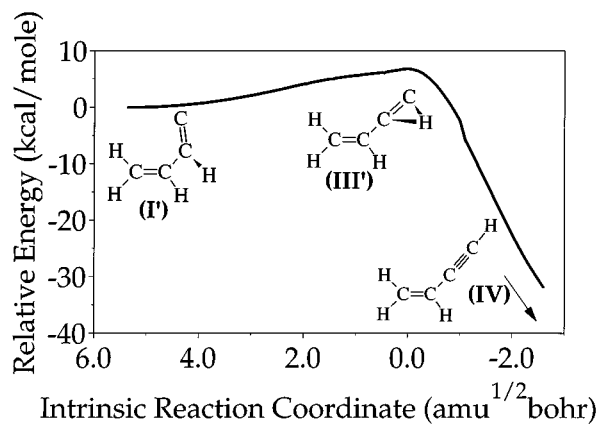


FIG. 6. Total RHF/D95(*d,p*) energy along the intrinsic reaction coordinate.

The  $C_4H_4$  spectrum was simulated using parameters scaled appropriately from the  $C_4D_4$  simulation; no further empirical adjustments were attempted. The frequencies were taken as the same percentage of the CISD calculations as they had been in the deuterated case (e.g., 93% for the higher-frequency modes and 70% for  $\nu_2$ ). The displacements were scaled by the square root of the ratio of reduced masses  $R_i$  in the analogous modes. Vibrational temperatures were assumed to be the same for all modes, and were adjusted for a best fit within reasonable experimental values (300–450 K), at 300 K. The adiabatic electron affinity and the FWHM are the only other empirically adjusted parameters. Table V contains the calculated and adjusted parameters used in the  $C_4H_4$  simulation. The results for the spectrum are depicted in Fig. 4; further discussion of the singlet spectrum is deferred to Sec. IV.

### 3. Intrinsic reaction coordinate

The RHF and CISD geometry calculations on the neutral potential energy surface show that, like the anion, singlet vinylvinylidene (**I**) is a planar molecule in a trans configuration. In the transition state, however, the migrating hydrogen atom has swung out of plane and is closer to a cis conformation than to the original trans state (**III'**, Fig. 1). In the product vinylacetylene, of course, this hydrogen atom is collinear with the three adjacent carbons so the dihedral angle becomes ill defined. The  $H_2CC$  system does not undergo this out-of-plane bend on the singlet surface,<sup>4</sup> but an exploration<sup>19</sup> of the vinylidene triplet surface revealed that it goes through a transition state very similar to **III'**; the triplet vinylidene transition state has a dihedral angle of 79°.

The complexity of the  $C_4H_4$  singlet surface can be illustrated using an intrinsic reaction coordinate (IRC) calculation. The IRC starts at the nonplanar transition state **III'** and follows the reaction path in small steps to singlet vinylvinylidene on one side and vinylacetylene on the other side. This calculation was limited to the RHF level of theory because a CISD study would have been prohibitively expensive and the trends do not change significantly between the RHF and CISD levels. The energy along the IRC is pictured in Fig. 6.

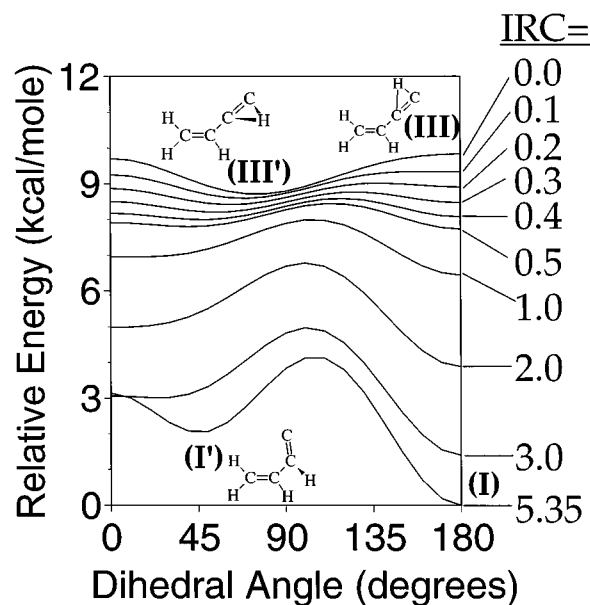


FIG. 7. Dependence of the vinylvinylidene RHF/D95(*d,p*) total energy on CC single bond rotation for several points along the IRC from IRC=0 (transition state) to IRC=5.35 (singlet vinylvinylidene).

This reaction path calculation starts at the out-of-plane transition state and follows the reaction path until it arrives at a nonplanar singlet vinylvinylidene similar to **I'** in Fig. 1. This structure is a second singlet vinylvinylidene with a dihedral angle of 48°. The potential energy surface between singlet vinylvinylidene **I'** and the transition state **III'** was examined by performing single-point RHF energy calculations with the bond lengths and angles frozen at their values at several points along the reaction path. At each point along the path the dihedral angle was rotated through regular intervals to obtain a three-dimensional picture (energy, reaction path, and dihedral angle) as shown in Fig. 7. The minimum at 180° is lower in energy than the nonplanar minimum except at points very close to the transition state. This minimum disappears completely near an IRC of ~0.1, leaving only one minimum at the transition state structure itself, with a dihedral angle of 75° (RHF-optimized value), or 68° (CISD-optimized value).

Careful examination of Fig. 7 is necessary in order to understand the reaction path in the vinylvinylidene system. First, upon examining the curves one sees that, while there is a clear minimum with a dihedral angle of ~50°–70° at the transition state structure **III'** and at the structure **I'**, this energy minimum seems to move to a dihedral angle of 0° for intermediate points along the path. This is an artifact of the calculation brought about because, when all bond lengths and angles are frozen while rotating the dihedral angle, the movement is not precisely perpendicular to the reaction path.

Second, the energy minimum at 180° does not disappear until very close to the transition state. Since the bond lengths and angles are frozen at values along the IRC, where the dihedral angle is consistently 50°–70°, and rotation about the single bond is not perpendicular to the IRC, this minimum could also be an artifact due to symmetry. It is surprising,

therefore, that it disappears near the transition state, forming a saddle point of order 2 rather than a “normal” transition state (i.e., two imaginary frequencies rather than one). Geometry optimizations of structure **III** at the RHF and CISD levels, with subsequent frequency calculations, have confirmed that this is a genuine saddle point of order 2 at these levels. However, very recent, higher level calculations by Walch and Taylor<sup>28</sup> result in a planar transition state with only one imaginary frequency. The potential energy surface in this region, therefore, may be further clarified by even more extensive calculations.

The IRC calculations also elucidate the position of the transition state along the reaction path relative to the singlet vinylvinylidene (**I**) and vinylacetylene (**IV**) structures. In vinylacetylene, the end hydrogen and the first three carbons are collinear, since two of the carbons are joined by a triple bond. In structure **I**, though, the carbons are all *sp*<sup>2</sup>-hybridized so that all of their bond angles are close to 120°. The transition state structure has a nearly linear CCC bond, and the migrating hydrogen is closer to the end carbon atom than the second, from which it started. This is a “late” transition state; it appears closer to the product vinylacetylene than to the reagent. This picture follows the same trend as in other vinylidene systems. Another similarity<sup>4,5</sup> to the vinylidene systems appears when correlation effects are included in the calculations: the transition state shifts towards the reactant side (“earlier” transition state) relative to the calculations which do not include electron correlation.

#### IV. DISCUSSION OF THE $\tilde{X}^1A'$ STATE SPECTRUM

The peaks in the  $\tilde{X}^1A'$  state, shown in Fig. 4, are approximately four times as wide as those in the  $\tilde{a}^3A'$  spectrum. Assigning these peaks, and the contributions to their widths, is the most interesting and difficult task in evaluating the vinylvinylidene system, and can be accomplished partially with additional information from the triplet state spectrum and the *ab initio* calculations.

First, the 52 meV of peak width needs to be deconvoluted into its component parts. Three processes can contribute to peak broadening beyond the instrumental resolution in photoelectron spectra: rotational broadening, vibrational congestion, and lifetime broadening. Each of these issues will be addressed in turn below.

##### A. Rotational broadening

The electron kinetic energy resolution of the photoelectron spectrometer is 5–6 meV, or 40–50 cm<sup>-1</sup>. This is sufficient to resolve most vibrational peaks (in the absence of extensive congestion), but leaves rotations unresolved. The result is that a rotational contour simply broadens the vibrational peaks in the photoelectron spectrum.

The *ab initio* calculated geometries of the vinylvinylidene anion and neutral yield *A*, *B*, and *C* rotational constants which can be used, together with the appropriate selection rules, to generate an approximate rotational spectrum for a transition from the anion to the neutral. This calculation was carried out with the  $\tilde{a}^3A'$  and the  $\tilde{X}^1A'$  states, using a rotational temperature equal to that found in the vinylidene study<sup>2</sup> of 150 K. No major differences between the peak

shapes corresponding to the two transitions were found, despite the differing selection rules for the two states (since the extra electron comes out of an orbital approximately perpendicular to the *A* axis to form the singlet, the selection rules are roughly those for a perpendicular transition; the electron is ejected from a more parallel orbital to form the triplet resulting in a roughly parallel type transition). When each component in the calculated rotational spectrum is convoluted with a 6-meV-wide Gaussian function corresponding to the instrumental response, the simulation results in a maximum peak width of 15 meV for the origins of both the singlet and the triplet states in C<sub>4</sub>H<sub>4</sub>, and 11 meV for the singlet C<sub>4</sub>D<sub>4</sub>. The 15 meV is very close to the observed width in the  $\tilde{a}^3A'$  state origin, indicating that rotational broadening is the major component in the triplet peak widths. However, the origin band in the singlet spectrum is much broader than 15 meV, so other factors must contribute.

The differences and similarities in the rotational contours calculated for vinylidene and for vinylvinylidene are important to note. The triplet states of the two molecules have approximately the same peak widths, and in both cases this width can be attributed to rotational broadening. But the widths of the singlet state peaks in vinylidene are only twice those of the triplet as opposed to a factor of 4 in vinylvinylidene, and the smaller size and greater symmetry of vinylidene make the rotational contribution for the singlet much greater<sup>2</sup> than in vinylvinylidene. The extra width in the singlet, therefore, is almost entirely attributed to rotational broadening in vinylidene. The vinylvinylidene system involves not only a larger and more asymmetric molecule but also dramatically wider peak widths in the singlet spectrum, meaning that rotation is a relatively minor contributor to the singlet peak widths. A substantial contribution from vibrational congestion and/or lifetime broadening must be present to form such wide peaks.

##### B. Vibrational congestion

While the treatment of rotational broadening in vinylvinylidene was simpler than in vinylidene because the molecule is larger and more asymmetric, the same factors make analysis of the vibrations in vinylvinylidene more complicated. Vinylidene has six distinct vibrations, half of which are totally symmetric and therefore symmetry allowed in photoelectron spectroscopy. Even with so few vibrations, of course, a detailed analysis was necessary to interpret the vinylidene photoelectron spectrum. Vinylvinylidene, with twice as many atoms and a lowered symmetry, contains 18 vibrational modes of which 13 are totally symmetric. Considerable help is needed, therefore, to locate and identify the vibrations in the singlet state vinylvinylidene spectrum. The *ab initio* calculations reported here have provided much of the necessary additional information.

First, the frequencies which the photoelectron spectrometer can resolve need to be determined. Looking at the triplet spectrum again, it is apparent that vibrations separated by 140 cm<sup>-1</sup> are easily distinguished from one another, and the rotational broadening is approximately equal for the singlet and triplet states. Therefore, in the absence of lifetime broadening, any two peaks separated by at least 200 cm<sup>-1</sup> are

resolvable in the singlet state. But no peaks are resolved at all within the 52 meV ( $420\text{ cm}^{-1}$ ) FWHM origin peak in the singlet spectrum. Therefore the search for active low-frequency vibrations responsible for lifetime broadening and/or vibrational congestion can be limited to those of less than  $200\text{ cm}^{-1}$ .

According to the CISD calculations there are only two vibrations with frequencies below  $200\text{ cm}^{-1}$ , and the first is an out-of-plane mode. Since modes which are not totally symmetric are symmetry forbidden, the first mode can only be active in even quanta of excitation, effectively doubling the observable frequency to approximately  $314\text{ cm}^{-1}$ . Only one mode below  $200\text{ cm}^{-1}$  is left,  $\nu_2$  calculated at  $197\text{ cm}^{-1}$  in  $\text{C}_4\text{H}_4$  and  $187\text{ cm}^{-1}$  in  $\text{C}_4\text{D}_4$ . This can be described as a  $\text{C}_1\text{C}_2\text{C}_3$  bend, and it is analogous to the isomerization coordinate (the CCF bend) found as part of the previous fluorovinylidene study.<sup>3</sup>

Examination of Tables III, IV, and V reveals that the parameters entering the Franck–Condon simulations included in Fig. 4 are very close to the original calculated values. The frequencies have not been adjusted beyond the normal 7% scaling of CISD frequencies, with the exception of the anharmonic and low-frequency  $\nu_2$ . The calculated anharmonicities for all modes except  $\nu_2$  are quite small and so were neglected. Harmonic oscillator wave functions were used for the higher modes to simulate Franck–Condon overlaps while Morse oscillator wave functions were used for  $\nu_2$ . Vibrational frequencies of the anion were assumed to be equal to the corresponding vibrations in the singlet except for  $\nu_2$ , where the value found in the triplet state spectrum ( $250\text{ cm}^{-1}$ ) was used. Only the displacements, the FWHM, and the frequency of  $\nu_2$  were adjusted empirically to arrive at the simulations appearing in Fig. 4.

By using the calculations to reduce the number of parameters in the simulation a FWHM for the peaks in the photoelectron spectrum can be extracted. The most successful fit (Table III and Fig. 4) finds a FWHM of 18 meV in  $\text{C}_4\text{H}_4$  and 17 meV in  $\text{C}_4\text{D}_4$ , greater widths than the 15 and 11 meV of rotational broadening convoluted with instrumental resolution estimated above for  $\text{C}_4\text{H}_4$  and  $\text{C}_4\text{D}_4$ , respectively, and as observed for the  $\tilde{a}^3A'$  state of  $\text{C}_4\text{H}_4$ . Since the simulation takes vibrational congestion into account as well, the only remaining contribution to the widths of these peaks must be lifetime broadening.

A range of widths was employed to determine the range of reasonable lifetimes. The simulation of the  $\text{C}_4\text{H}_4$  singlet spectrum presented in Fig. 4 (FWHM=18 meV) provides a minimum peak width since narrower lines do not provide a satisfactory fit even with a greatly reduced frequency in  $\nu_2$ . The spectrum can be simulated relatively well with peak widths up to 50 meV, though this requires unrealistic frequencies and displacements of the vibrations. The minimum lifetime is not well determined, since the maximum peak width is unclear; however, the maximum possible lifetime of singlet vinylvinylidene is given by the 18 meV simulation.

### C. Lifetime broadening

Photoelectron spectroscopy is, to a first approximation, a probe of the slope of the neutral potential energy surface in

the region of Franck–Condon overlap with the anion vibrational ground state. Therefore, while an estimate of the lifetime broadening in the spectrum is obtainable through careful analysis, further analysis of the consequences of this broadening is speculative. An observation of the lifetime broadening is given below, therefore, and further discussion presented only as a preliminary analysis.

The lifetime of singlet vinylvinylidene can be estimated by subtracting the effects of rotational broadening, vibrational congestion, and instrumental resolution from the total widths of the photoelectron spectrum peaks. The Franck–Condon simulation removes the effects of vibrational congestion from the line shapes by producing a separate (18-meV-wide) peak for each vibrational transition. A rough approximation of the lifetime broadening is simply the FWHM in the simulation minus 15 meV (the instrumental plus rotational broadening). This leaves 3 meV of lifetime broadening in the singlet vinylvinylidene photoelectron spectrum. Similarly, the simulation of the  $\text{C}_4\text{D}_4$  spectrum is most successful with 17 meV peak widths and our estimate of instrumental and rotational broadening is 11 meV, leaving 6 meV attributable to lifetime broadening. The difference in lifetimes between  $\text{C}_4\text{H}_4$  and  $\text{C}_4\text{D}_4$ , however, is probably insignificant compared to the errors introduced by the approximations made to arrive at these lifetimes; therefore the best guess at the lifetime broadening in the singlet vinylvinylidene spectrum (deuterated or not) is 3–6 meV. A brief evaluation of the significance of this parameter is presented below.

Using the equation

$$W_{1/2} = \frac{1}{2\pi c\tau}, \quad (6)$$

where  $W_{1/2}$  is the FWHM attributed to lifetime broadening and  $\tau$  is the time constant of a single exponential decay, the lifetime estimate of singlet vinylvinylidene is  $\tau \approx 0.1\text{--}0.2\text{ ps}$ .

An absolute minimum to the lifetime of singlet vinylvinylidene can be obtained from the simulations with a maximum peak width. If 50 meV is taken as the maximum peak width in the  $\text{C}_4\text{H}_4^-$  spectrum, then the maximum  $W_{1/2}=35\text{ meV}$  and the minimum lifetime is 20 fs.

It is instructive to compare the Franck–Condon simulations further with the data. The  $\text{C}_4\text{D}_4$  singlet spectrum is well accounted for by the simulation, partially as a result of empirical adjustments. The peaks in the  $\text{C}_4\text{H}_4$  spectrum, however, are apparently more difficult to account for; only the first two peaks display a good match between data and simulation and a large gap appears between the first and second peaks. Several fits of the  $\text{C}_4\text{H}_4$  spectrum were attempted independent of the  $\text{C}_4\text{D}_4$  simulation, varying the displacements of all modes listed in Tables IV and V. The portions of the  $\text{C}_4\text{H}_4$  spectrum in question were impossible to account for without straying too far afield of the calculations to be physically meaningful. There are several possible explanations for this extra intensity in the spectrum: (1) the potential energy surface is very irregular so that a harmonic potential is inadequate to describe it along one or more of the vibrations; (2) the anharmonicity in one or more modes is much larger than calculated; (3) the vibrations do not act as independent har-

monic oscillators, instead mixing in some way with one another (possibly with an energy dependence to the mixing); (4) one or more out-of-plane modes is active in the spectrum, a possibility supported by the nonplanar structure of the transition state; or (5) the lifetime broadening has an energy dependence so that the effective width of the peaks is increased with increasing internal energy in the singlet. Though any or all of these factors could contribute, the information available through the Franck–Condon simulation is insufficient to distinguish one from another. The simple interpretation of spectra of dissociative molecular states presented by Pack<sup>10</sup> also may be important for explaining photoelectron spectra of 1,2-hydrogen shift systems such as vinylvinylidene.

Another useful exercise is to compare the lifetime estimate of vinylvinylidene to that of vinylidene. The best estimate of the lifetime broadening present in the vinylidene photoelectron spectrum<sup>2</sup> is 3 meV, identical to the figure obtained in vinylvinylidene. Though the lifetime broadening in the fluorovinylidene spectrum<sup>3</sup> was not extracted, it is probably not significantly different from that of vinylidene and vinylvinylidene. This similarity indicates that the slopes of the potential energy surfaces, in the region of Franck–Condon overlap with the corresponding anions, are *approximately the same* despite a relatively wide variation of the substituents and a resultant variation in the electron affinities and normal coordinate displacements. The potential energy surface may be strongly affected by such a change in other regions, such as closer to the transition state to isomerization, but photoelectron spectroscopy cannot elucidate these differences. The apparently equivalent lifetimes of singlet vinylidene, fluorovinylidene, and vinylvinylidene provide an interesting clue to the behavior of rapidly evolving systems: The shapes of the potential energy surfaces, and their absolute positions relative to those of the anions, may be very different from one another, but in the region of Franck–Condon overlap between anion and neutral the slopes are governed primarily by the presence of the vinylidene group.

## V. CONCLUSION

The negative-ion photoelectron spectra of vinylvinylidene and vinylvinylidene-*d*<sub>4</sub> anions have been presented along with *ab initio* calculations to aid in the interpretation of the spectra. The electron affinity of vinylvinylidene has been reported along with singlet–triplet splittings between the ground state and the first two triplet states of vinylvinylidene. The anisotropy parameters of the  $\tilde{X}^1A'$  state and the  $\tilde{a}^3A'$  state have been measured, and the anisotropy parameter of the  $\tilde{b}^3A''$  state was estimated. Several vibrational frequencies were reported for the  $\tilde{a}^3A'$  state, and several  $\tilde{X}^1A'$  frequencies were reported with the aid of the *ab initio* calculations.

By combining our photoelectron spectra with *ab initio* calculations, we have estimated the lifetime of singlet vinylvinylidene to be 20–200 fs. These values were extracted by separating the effects of instrumental resolution, rotational broadening, and vibrational congestion from the lifetime broadening. Calculations have provided equilibrium geometries of seven distinct stationary points at the CISD level.

This includes two anion configurations separated by a cis-trans isomerization, two singlet vinylvinylidene structures, and two hydrogen shift transition structures, each pair differing by the same CC single bond rotation, and the vinylacetylene structure. The geometry calculations also provide relative energies of the five singlet structures, and the cis-trans isomerization energy of the vinylvinylidene anion.

An important clue to the behavior of these types of systems is provided by the remarkable similarity of the lifetimes of vinylidene and vinylvinylidene. The potential energy surfaces of the singlet surfaces of these systems are very similar near the anion geometries; however, they diverge from one another in other regions, possibly even near the 1,2-hydrogen-shift isomerization barrier. The potential energy surface of the vinylvinylidene system, in particular, is extremely complex and makes up only a small portion of the C<sub>4</sub>H<sub>4</sub> surface. More study of this surface is certainly possible and will provide extensive additional information about short-lived species, transition states, and the evolution of wavepackets along potential energy surfaces. Since a wave packet simulation along the isomerization coordinate may better describe the photoelectron spectrum, one of the authors (H.K.) intends to perform such calculations in the near future.

## ACKNOWLEDGMENTS

This work was supported by National Science Foundation Grants No. PHY90-12244 and CHE93-18639. Helpful conversations with G. Barney Ellison, S. P. Walch, and E. J. Heller are gratefully acknowledged. The authors would like to thank the Visiting Fellowship Program of the National Institute for Standards and Technology and the Joint Institute for Laboratory Astrophysics for generously providing computer time for the calculations presented here.

- <sup>1</sup> See, for example, D. M. Neumark, *Acc. Chem. Res.* **26**, 153 (1993).
- <sup>2</sup> K. M. Ervin, J. Ho, and W. C. Lineberger, *J. Chem. Phys.* **91**, 5974 (1989).
- <sup>3</sup> M. K. Gilles, W. C. Lineberger, and K. M. Ervin, *J. Am. Chem. Soc.* **115**, 1031 (1993).
- <sup>4</sup> M. M. Gallo, T. P. Hamilton, and H. F. Schaefer III, *J. Am. Chem. Soc.* **112**, 8714 (1990).
- <sup>5</sup> B. J. DeLeeuw, J. T. Fermann, Y. Xie, and H. F. Schaefer III, *J. Am. Chem. Soc.* **115**, 1039 (1993).
- <sup>6</sup> J. F. Stanton and J. Gauss, *J. Chem. Phys.* **101**, 3001 (1994).
- <sup>7</sup> G. Herzberg, *Electronic Spectra and Electronic Structure of Polyatomic Molecules* (Van Nostrand Reinhold, New York, 1966), Chaps. 4 and 5.
- <sup>8</sup> J. W. Rabalais, J. M. McDonald, V. Scherr, and S. P. McGlynn, *Chem. Rev.* **71**, 73 (1971).
- <sup>9</sup> R. D. Hudson, *Rev. Geophys. Space Phys.* **9**, 305 (1971).
- <sup>10</sup> R. T. Pack, *J. Chem. Phys.* **65**, 4765 (1976).
- <sup>11</sup> H. F. Schaefer III, *Acc. Chem. Res.* **12**, 288 (1979).
- <sup>12</sup> G. C. Goode and K. R. Jennings, *Adv. Mass. Spectrom.* **6**, 797 (1974).
- <sup>13</sup> J. H. H. Dawson and N. M. M. Nibbering, *J. Am. Chem. Soc.* **100**, 1928 (1978).
- <sup>14</sup> J. Chandrasekhar, R. A. Kahn, and P. v. R. Schleyer, *Chem. Phys. Lett.* **85**, 493 (1982).
- <sup>15</sup> C. E. Dykstra and H. F. Schaefer III, *J. Am. Chem. Soc.* **100**, 1378 (1978).
- <sup>16</sup> Y. Osamura, H. F. Schaefer III, S. K. Gray, and W. H. Miller, *J. Am. Chem. Soc.* **103**, 1904 (1981).
- <sup>17</sup> G. Frenking, *Chem. Phys. Lett.* **100**, 484 (1983).
- <sup>18</sup> L. B. Harding, *J. Am. Chem. Soc.* **103**, 7469 (1981).
- <sup>19</sup> M. P. Conrad and H. F. Schaefer III, *J. Am. Chem. Soc.* **100**, 7820 (1978).
- <sup>20</sup> R. Krishnan, J. J. Frisch, J. A. Pople, and P. v. R. Schleyer, *Chem. Phys. Lett.* **79**, 408 (1981).

- <sup>21</sup>S. M. Burnett, A. E. Stevens, C. S. Feigerle, and W. C. Lineberger, *Chem. Phys. Lett.* **100**, 124 (1983).
- <sup>22</sup>T. Carrington, Jr., L. M. Hubbard, H. F. Schaefer III, and W. H. Miller, *J. Chem. Phys.* **80**, 4347 (1984).
- <sup>23</sup>C.-H. Hu and H. F. Schaefer III, *J. Phys. Chem.* **97**, 10681 (1993).
- <sup>24</sup>C. L. Collins, C.-H. Hu, Y. Yamaguchi, and H. F. Schaefer III, *Isr. J. Chem.* **33**, 317 (1993).
- <sup>25</sup>B. Ma and H. F. Schaefer III, *J. Am. Chem. Soc.* **116**, 3539 (1994).
- <sup>26</sup>C. Richards, C. Meredith, S.-J. Kim, G. E. Quelch, and H. F. Schaefer III, *J. Chem. Phys.* **100**, 481 (1994).
- <sup>27</sup>M. J. Travers, D. C. Cowles, E. P. Clifford, G. B. Ellison, and P. C. Engelking, *J. Chem. Phys.* (to be published).
- <sup>28</sup>S. P. Walch and P. R. Taylor (private communication).
- <sup>29</sup>H. Kollmar, F. Carrion, M. J. S. Dewar, and R. C. Bingham, *J. Am. Chem. Soc.* **103**, 5292 (1981).
- <sup>30</sup>M.-Y. Zhang, C. Wesdemiotis, M. Marchetti, P. O. Danis, J. C. Ray, B. K. Carpenter, and F. W. McLafferty, *J. Am. Chem. Soc.* **111**, 8341 (1989).
- <sup>31</sup>B. A. Hess, W. D. Allen, D. Michalska, L. J. Schaad, and H. F. Schaefer III, *J. Am. Chem. Soc.* **109**, 1615 (1987), and references therein.
- <sup>32</sup>D. W. Kohn and P. Chen, *J. Am. Chem. Soc.* **115**, 2844 (1993).
- <sup>33</sup>R. F. Gunion, M. K. Gilles, M. L. Polak, and W. C. Lineberger, *Int. J. Mass Spec. Ion Proc.* **117**, 601 (1992).
- <sup>34</sup>L. W. Tutt, D. Tannor, J. Schindler, E. J. Heller, and J. I. Zink, *J. Phys. Chem.* **87**, 3017 (1983); L. W. Tutt, J. I. Zink, and E. J. Heller, *Inorg. Chem.* **26**, 2158 (1987).
- <sup>35</sup>D. G. Leopold, K. K. Murray, A. E. Stevens Miller, and W. C. Lineberger, *J. Chem. Phys.* **83**, 4849 (1985).
- <sup>36</sup>K. M. Ervin and W. C. Lineberger, in *Advances in Gas Phase Ion Chemistry Vol. 1*, edited by N. G. Adams and L. M. Babcock (JAI, Greenwich, CT, 1992), pp. 121–166.
- <sup>37</sup>J. Lee and J. J. Grabowski, *Chem. Rev.* **92**, 1611 (1992).
- <sup>38</sup>J. H. J. Dawson and K. R. Jennings, *J. Chem. Soc. Faraday Trans. 2* **72**, 700 (1976).
- <sup>39</sup>P. K. Chou and S. R. Kass, *J. Am. Chem. Soc.* **113**, 697 (1991), and private communications with the authors.
- <sup>40</sup>GAUSSIAN 92, Revision E.2, M. J. Frisch, G. W. Trucks, M. Head-Gordon, P. M. W. Gill, M. W. Wong, J. B. Foresman, B. G. Johnson, H. B. Schlegel, M. A. Robb, E. S. Replogle, R. Gomperts, J. L. Andres, K. Raghavachari, J. S. Binkley, C. Gonzalez, R. L. Martin, D. J. Fox, D. J. Defrees, J. Baker, J. J. P. Stewart, and J. A. Pople (Gaussian, Inc., Pittsburgh, PA, 1992).
- <sup>41</sup>J. Cooper and R. N. Zare, *J. Chem. Phys.* **48**, 942 (1968); **49**, 4252 (1968); J. L. Hall and M. W. Siegel, *ibid.* **48**, 943 (1968); D. Hanstorp, C. Bengtsson, and D. J. Larson, *Phys. Rev. A* **40**, 670 (1989).